Mixing of viscous immiscible liquids. Part 2: Overemulsification—interpretation and use

P. DeRoussel[a], D. V. Khakhar[b], J. M. Ottino[a, *]

[a] *Department of Chemical Engineering, Robert McCormick School of Engineering, Northwestern University, 2145 Sheridan Road, Evanston, IL 60208-3120, USA*

[b] *Department of Chemical Engineering, Indian Institute of Technology—Bombay Powai, Bombay 400076, India*

Abstract

In mixing of immiscible fluids, the final steady state drop size distribution, corresponding to a minimum mean drop size, is commonly approached in a monotonic way. There are, however, other scenarios. Overemulsification refers to cases where, (I) after reaching a minimum, the average size increases and then levels off to a final size, or (II) the average size oscillates. In case (I) the drop size distribution becomes bimodal after the average size goes through a minimum; gradually, the peak at smaller sizes moves towards the peak at larger sizes resulting in a narrow distribution. An explanation of this phenomenon is offered and ways to exploit it are suggested.

Keywords: Mixing; Dispersion; Liquids; Polymer processing; Drop size distributions; Overemulsification

1. Introduction

The physical properties of mixtures of immiscible liquids are determined by the structure—size and distribution of phases—of the mixture. For example, the impact strength of a polymer blend, obtained after quenching the melt-interspersion obtained from a mixing process, is a function of its morphology. Similarly, the rheology of food and home care products is a function of the drop size distribution.

Mixing processes lead to complex time-dependent drop size distributions, typically evolving from a narrow coarse distribution of large fluid blobs to a wide distribution of small drops. The final drop size is the result of the competition between fluid stretching and breakup, which decreases the average size, and coalescence, which increases the average size. The typical picture for the case of a batch (or internal) mixer is as follows: The average drop size decreases over time (t) and levels off to a final size with further mixing, resulting in no noticeable size reduction (Case 1 in Fig. 1). Similar comments can be made about continuous mixers, e.g. extruders or static mixers, if the fluid mechanical action remains constant along the flow path z. Thus, in what follows t and z are regarded as equivalent.

There is, however, the possibility that the final steady state size may *not* be the minimum size or that the steady state may correspond to periodic oscillations. This phenomenon is called *overemulsification*, and is illustrated in Fig. 1. Two scenarios are possible: (I) after reaching a minimum the average size increases and levels off to a final size (Case 3 of Fig. 1) or, (II) the average size oscillates (Case 2 of Fig. 1). There are also associated changes in the drop size distribution, becoming bimodal after the average size goes through a minimum. Gradually, the peak at smaller sizes moves to the peak at larger sizes resulting in a narrow distribution at the end of mixing.

The first reference to overemulsification in the literature appears to be the work of Becher (1967). In Becher's experiments, a homogenizer was used to create an oil–chlorobenzene-surfactant emulsion. Experiments revealed that if processing continued beyond a certain point, the average size of the dispersed phase would increase. This phenomenon appears to be relatively unknown in the polymer processing community though one

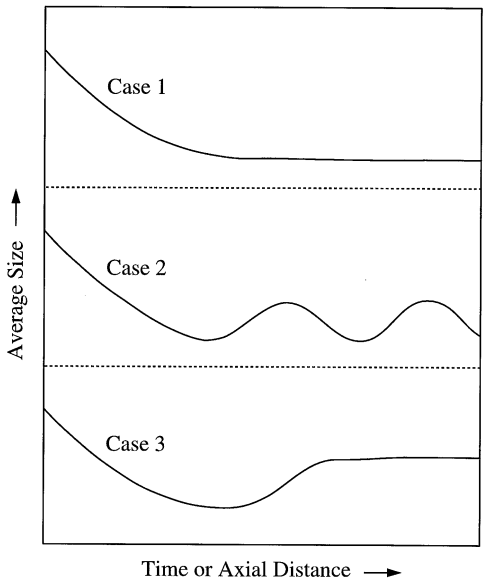

Fig. 1. Illustration of the change in average size during a mixing process. Case 1 corresponds to the typical case of a monotonic decrease in the average size. Case 2 corresponds to overemulsification in which the average size of the distribution oscillates. Case 3 corresponds to overemulsification in which a final steady state is reached.

may imagine ways in which it could be used. In fact, Thalacker (1998) (personal communication to DeRoussel) observed overemulsification in extrusion of a polymer blend and Adewole, Wolkowicz, Mascia, and Gogos (1998) showed an increase in the average size of the dispersed phase of a compatibilized PP–PS blend. In the latter case, however, the increase occurred *after* the mixing section of the extruder and it is not clear if this is due to a change in the flow conditions or if it was indeed a case of overemulsification.

Computational models have also predicted this phenomenon. The models of Becher and McCann (1991) Becher and McCann (1990) and Lachaise, Mendiboure, Dicharry, Marion, and Salager (1996) predict overemulsification in stirred tanks. A third model, by DeRoussel, Khakhar, and Ottino (2001), developed for low Reynolds number mixing of two immiscible viscous liquids in an internal mixer (Mixing I model) also predicts this phenomenon. Fig. 2 shows two typical examples using this model. The volume average size is displayed versus time and the actual drop distribution and variance are shown at regular intervals. Fig. 2a shows the presence of a bimodal distribution as the average size increases and a narrow distribution in the final state. Fig. 2b shows an example with oscillations. In this case, a bimodal distribution is not as clear as the two peaks slightly overlap.

Is there a simple explanation of these results? Here we propose a qualitative explanation in terms of three length scales, $R_{\mathrm{def,min}}$, $R_{\mathrm{break,max}}$, and $R_{\mathrm{coal,max}}$ (to be defined shortly) and how they interplay and vary as a function of material and process parameters. The process

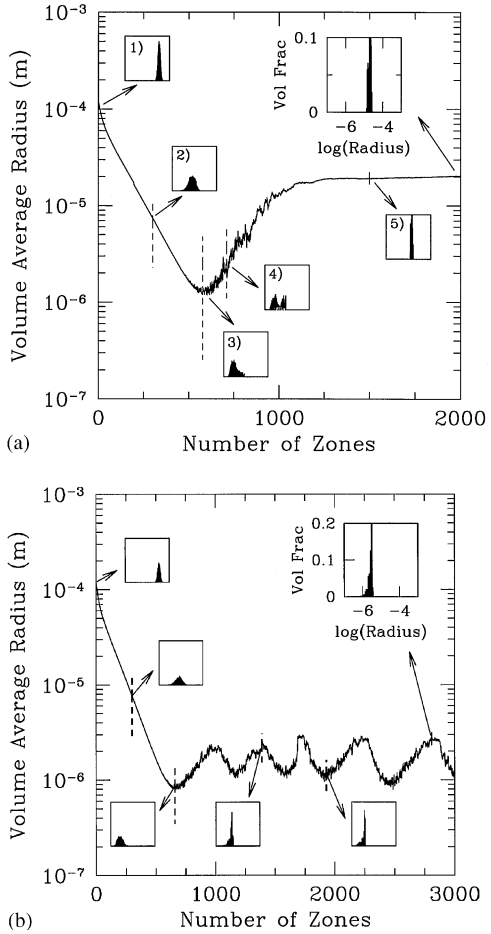

Fig. 2. Simulation results using the Mixing I model (DeRoussel et al., 2001) in which overemulsification is seen. The volume average radius is plotted versus time. The vertical dashed lines correspond to the standard deviation of the distribution. The actual distribution is also shown at various points. (a) Corresponds to Case 2 of Fig. 1. ($\mu_c = 1$ Pa s, $\mu_d = 1000$ Pa s, $\sigma = 5 \times 10^{-3}$ N/m, $\phi = 0.05$) (b) Corresponds to Case 3 of Fig. 1. ($\mu_c = 10$ Pa s, $\mu_d = 1000$ Pa s, $\sigma = 5 \times 10^{-3}$ N/m, $\phi = 0.05$).

parameters are: the viscosity of the continuous phase μ_c, the viscosity of the dispersed phase μ_d, and the shear rate $\dot{\gamma}$, which can be combined into two parameters, $\mu_c\dot{\gamma}/\sigma$ and μ_d/μ_c.

The analysis is based on the model described in DeRoussel et al. (2001); review aspects are therefore reduced to a minimum. The practical application of these results is that overemulsification can potentially be used to design mixing processes leading to more uniform distributions of drop sizes.

2. Definitions

The final drop size distribution of a mixing process is the balance between fluid stretching and breakup, on one hand, and coalescence, on the other. Initially, the

global character of the flow controls mixing with interfacial forces playing no role. However, as mixing proceeds interfacial forces become more dominant and stretching, breakup, and coalescence at drop length-scales become important.

The stability of a single drop in a linear flow depends on the viscosity ratio (p), the ratio of viscous forces to interfacial forces or capillary number (Ca), and the flow type (Taylor, 1934; Grace, 1972). If Ca is greater than some critical value, $\mathrm{Ca}_{\mathrm{crit}}$, the drop is deformed and eventually breaks. If the stretching occurs at supercritical capillary numbers, say $\kappa\mathrm{Ca}_{\mathrm{crit}}$, with κ about 5 or greater for a shear flow, the drop is deformed affinely (Tjahjadi & Ottino, 1991; Elemans, Bos, Janssen, & Meijer, 1993; Janssen, 1993). Therefore, the minimum size drop that can be deformed affinely in a given flow, $R_{\mathrm{def,min}}$, is given by

$$\mathrm{Ca} = \frac{\mu_c \dot{\gamma} R_{\mathrm{def,min}}}{\sigma} = \kappa \mathrm{Ca}_{\mathrm{crit}}. \tag{1}$$

Once a drop is deformed into an extended thread, it eventually breaks. For the mixing flows considered here, the dominant breakup mechanism is capillary instabilities. This type of breakup occurs by the growth of thermal disturbances on the surface of the thread and the growth of these disturbances is dependent upon if the thread is being stretched or is at rest. The time for breakup of threads at rest can be estimated by linear stability theory (Tomotika, 1935).

$$t_{\mathrm{break}} = \frac{2\mu_c R_o}{\sigma \Omega_m} \ln\left(\frac{0.82 R_o}{\alpha_o}\right). \tag{2}$$

Here Ω_m is the dimensionless growth rate, which is dependent on p, and α_o is the amplitude of the initial disturbance. In general, stretching delays breakup, so threads at rest break first. Therefore, solving (2) for R_o gives the *maximum* size thread that will break, $R_{\mathrm{break,max}}$, in a given amount of time set equal to t_{break}.

Once extended threads are broken into drops, the smaller drops begin to interact with each other and may coalesce. Coalescence can be broken into three steps—approach/collision, film drainage, and rupture. For an analysis of the contribution of overemulsification, one needs to estimate the *maximum* size drop that can coalesce in a given amount of time in a given flow; this value is denoted $R_{\mathrm{coal,max}}$. The value of $R_{\mathrm{coal,max}}$ depends on the film drainage and rupture steps, which can be modelled using the approach of Chesters (1991).

The rate of the film drainage between the squeezed drops (with thickness h) depends on the *mobility* and *rigidity* of the interface and is given by (Chesters, 1991)

$$\text{rigid interfaces:} \quad -\frac{\mathrm{d}h}{\mathrm{d}t} \approx \frac{2hF}{3\pi\mu_c R_o^2}, \tag{3}$$

$$\text{fully mobile interfaces:} \quad -\frac{\mathrm{d}h}{\mathrm{d}t} \approx \frac{2\sigma h}{3\mu_c R_o}, \tag{4}$$

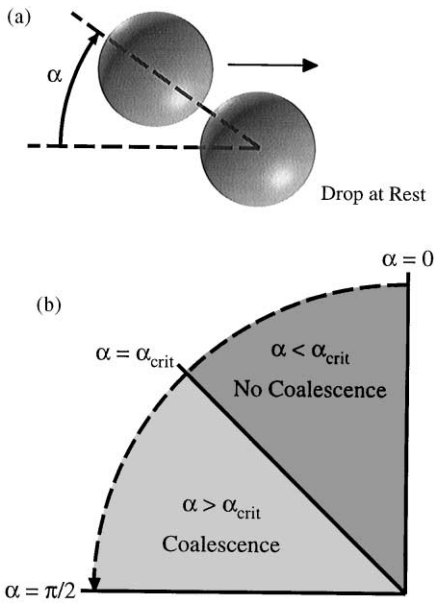

Fig. 3. (a) The collision angle α is the angle between the line tangent to the streamline on which a drop is moving and the line connecting the drop centers. (b) Coalescence will only occur for α_{init} less than the critical collision angle α_{crit}.

$$\text{partially mobile interfaces:} \quad -\frac{\mathrm{d}h}{\mathrm{d}t} \approx \frac{2(2\pi\sigma/R_o)^{3/2}h^2}{\pi\mu_d F^{1/2}}, \tag{5}$$

$$\text{immobile interfaces:} \quad -\frac{\mathrm{d}h}{\mathrm{d}t} \approx \frac{8\pi\sigma^2 h^3}{3\mu_c R_o^2 F}. \tag{6}$$

Here R_o is the drop radius and F is the driving force for film drainage. The value of the force F can be obtained as follows. As the film drains the drop rotates, the force driving the film drainage varies as (Allan & Mason, 1962)

$$F = 4.34\pi\mu_c\dot{\gamma}R_o^2 \sin 2\alpha, \tag{7}$$

$$\frac{\mathrm{d}\alpha}{\mathrm{d}t} = \dot{\gamma}(0.8\cos^2\alpha + 0.2\sin^2\alpha), \tag{8}$$

where α is the collision angle defined as the angle between the line tangent to the streamline on which a drop is moving and the line connecting the drop centers (see Fig. 3).

The time for two drops to coalesce is found by integrating the appropriate equation from (3) to (6) along with (7) and (8) from the initial film thickness to the final film thickness, h_{crit}.

$$h_{\mathrm{crit}} = \left(\frac{AR_o}{8\pi\sigma}\right)^{1/3}. \tag{9}$$

Therefore, an iterative procedure must be used to find $R_{\mathrm{coal,max}}$—Eqs. (3)–(9) are solved for the maximum size drop for which t_{drain} is less than the maximum time allowable for coalescence.

In order to complete the analysis, it is necessary to determine the probability that a collision will result in a successful coalescence event. Without loss of generality, when two drops collide, the initial collision angle, α_{init}, can be taken to be between 0 and $\pi/2$. The initial collision angle determines the amount of time available for film drainage. For any given set of conditions, there exists a critical initial collision angle, α_{crit}, below which coalescence will always occur and above which coalescence will never occur. So, for α_{crit} near $\pi/2$, coalescence is very probable. If we assume that all initial collision angles are equally probable, a coalescence probability can be defined as

$$P = \frac{\alpha_{crit}}{\pi/2}. \tag{10}$$

The critical angle, α_{crit}, is determined by using (2)–(9) to find the maximum angle for which coalescence will occur for a given size drop.

2.1. Simulations

The simulations presented in this paper are carried out using the Mixing I model (DeRoussel et al., 2001). This model accounts for stretching distributions and satellite formation; the specific model used here is based on the concept of dividing a mixer into two zones—strong and weak. The strong zone accounts for regions in which stretching and breakup during flow occurs; the weak zone accounts for coalescence and breakup occurring at rest. An initial distribution of drops is cycled through both zones and is evolved according to the fundamentals of stretching, breakup, and coalescence until a final distribution is obtained.

3. Overemulsification: a mechanism

We suggest that overemulsification can be understood in terms of the three critical radii defined above:

- $R_{def,min}$—the minimum size drop that can be deformed affinely by a given flow (see (1)).
- $R_{break,max}$—the maximum size thread that can break in a given flow in a given time (see (2)).
- $R_{coal,max}$—the maximum size drop that will coalesce in a given flow (see (3)–(9)). All these quantities are functions of the material properties (μ_c, μ_d, and σ) and the flow ($\dot{\gamma}$).

Consider the case illustrated in Fig. 4. The initial condition is a distribution of relatively large drops such that $Ca > \kappa Ca_{crit}$. The drops are stretched into extended threads and the size is reduced until $R_{break,max}$ is reached. At this point, the threads have exactly the radius that allows them to break in the allotted time. The threads break into a distribution of drops. These new drops are

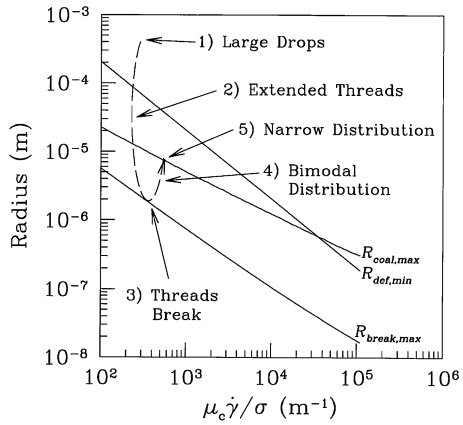

Fig. 4. Pictorial representation of the mechanism of overemulsification. The numbers correspond to those in Fig. 2a.

now below both $R_{coal,max}$ and $R_{def,min}$; therefore the drops begin to coalesce and the average size increases. Drops, however, cannot coalesce beyond $R_{coal,max}$, so the distribution becomes narrow as drops approach the value of $R_{coal,max}$.

Thus, based on the above arguments, a necessary condition for overemulsification is that both $R_{def,min}/R_{break,max}$ and $R_{coal,max}/R_{break,max}$ be larger than K, where K is a constant which is greater than one.

Grizzuti and Bifulco (1997) conducted experiments in which an emulsion with an initial condition corresponding to point 3 in Fig. 4 was sheared in a parallel plate apparatus. The final drop size varied with radial position—due to the radial dependence of shear rate—and corresponded with the line for $R_{coal,max}$. Even though these experiments are not a manifestation of overemulsification, they represent the same phenomena as the second part of the overemulsification mechanism and show the approach of the drop distribution to $R_{coal,max}$.

Besides the minimum in size and narrowing of the distribution, another characteristic of overemulsification is the bimodal distribution that occurs after the average size goes through a minimum (Fig. 2a). During the increase in size, drops from the peak at smaller sizes gradually move to the peak at larger sizes. Once the drops reach the peak at larger sizes, they can no longer coalesce. However, if $R_{coal,max} > R_{def,min}$, as drops reach larger sizes they will be stretched and the peak of drops at larger sizes never forms. This explains why overemulsification can only occur for $R_{coal,max} < R_{def,min}$. The second necessary condition for overemulsification is therefore $R_{coal,max} < R_{def,min}$.

For the example of Fig. 4 and the experiments of Grizzuti and Bifulco (1997), the shear rate dependence is well characterized (Grizzuti and Bifulco used a parallel plate apparatus) and the values of $R_{coal,max}$, $R_{def,min}$, and $R_{break,max}$ can be represented as lines. However, in any real mixer, there is a distribution of shear rates and the values for the critical radii are fuzzy *regions* around some

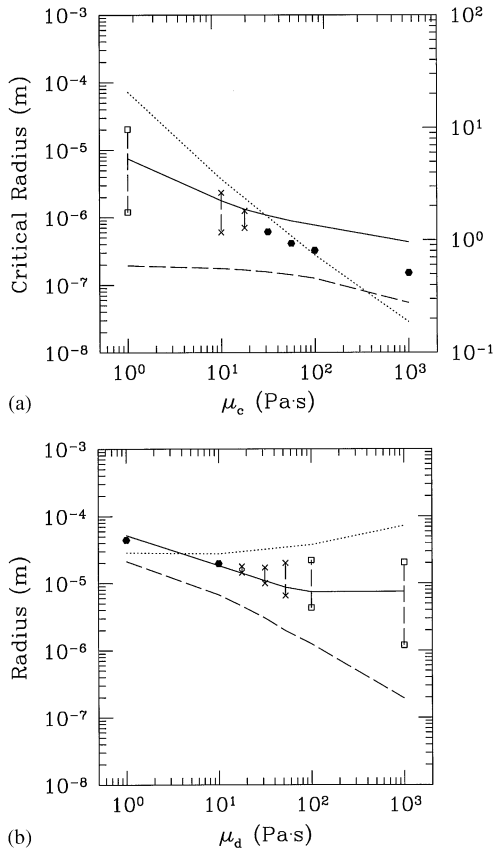

Fig. 5. Change in $R_{coal,max}$, $R_{def,min}$, and $R_{break,max}$ as (a) μ_d and (b) μ_c are varied. The points represent results from the Mixing I model. A single point (•) represents a simulation in which the average size decreased monotonically to a final steady state. The points connected by vertical lines represent simulations in which overemulsification occurs—the bottom point corresponding to the minimum size and the top point to the final steady state size or the maximum size of the oscillations (×—oscillation and □—steady state).

average line. If the region for $R_{coal,max}$ overlaps with the region for $R_{def,min}$, then drops can coalesce to the point that they will be deformed and stretched. Drops are continually stretched until they reach $R_{break,max}$, at which point they break again. This situation leads to the oscillatory behavior illustrated in Fig. 2b. Therefore, a necessary condition for overemulsification with oscillatory behavior is $1 < R_{def,min}/R_{coal,max} < B$, where B is a constant. Also, the condition for overemulsification that reaches a steady state can be written as $R_{def,min}/R_{coal,max} > B$.

In order to estimate a value for K, two illustrative simulations were run—one for which overemulsification did not occur and one in which it did. Other simulations were run at parameter sets (μ_c, μ_d, σ, and $\dot{\gamma}$) which gave values of $R_{def,min}/R_{break,max}$ and $R_{coal,max}/R_{break,max}$ between the first two simulations. Using this procedure, the transition to overemulsification can be found and a value of about 3 is obtained for K. A similar procedure was used to find the transition from overemulsification with oscillation to overemulsification with a steady state. For this case, the relevant parameter is $R_{def,min}/R_{coal,max} = B$. The value of B was found to be approximately 4.

Thus the key to controlling or predicting overemulsification is understanding how $R_{coal,max}$, $R_{def,min}$, and $R_{break,max}$ vary as material and process parameters are changed. Fig. 5 shows variation of the critical radii as μ_c, μ_d, σ, and $\dot{\gamma}$ are varied. Also, shown in Fig. 5 are results from the Mixing I model using different parameters. Simulations that do not show overemulsification (as in Case 1 in Fig. 1) are displayed as a single point. Those that display overemulsification are displayed as two points connected by a vertical line—the bottom point represents the size at which the minimum occurs and the top point represents the final size or maximum size of an oscillation.

As shown in Figs. 5a and b, high μ_d and low μ_c (high p) lead to conditions propitious for overemulsification. For example, in Fig. 5a as μ_c decreases from approximately 30 to 15 Pa s, the mixing changes from the steady state case without overemulsification to the oscillatory case with overemulsification. In addition, increasing σ and lowering $\dot{\gamma}$ will cause overemulsification.

4. Discussion

Often the ideal final outcome of a mixing process is a narrow distribution of small drops. For standard mixing processes, as the average size decreases the width of the distribution increases and then eventually decreases. In the standard case, the two important variables, size and standard deviation, are "moving in the right direction" at the end of the mixing process. Therefore, the most desirable state corresponds to steady state. For overemulsification, this is not as straightforward. The ideal case of small drop sizes *and* a narrow distribution is not attainable through overemulsification. Small sizes are sacrificed for a smaller width, or vice versa, depending on the intended application for the product being made. This leads to the question of optimum mixing time. Let us outline possible ways to estimate the optimum mixing time and examine the tradeoffs between size and variance that occur in overemulsification.

Fig. 6 plots the volume average radius versus the standard deviation of the distribution normalized by the average size for the simulation in Fig. 2a. The initial condition (point 1) is $R_{avg} \approx 100$ μm and $s/R_{avg} \approx 0.27$. As mixing begins the average size decreases and the width of the distribution increases—going through point 2 proceeding to point 3. At point 3, the minimum size is reached and the average size begins to increase as coalescence dominates the process. Due to the bimodal distribution, the width of the distribution also increases (point 4). Eventually the variance begins to decrease, becoming very small by the time the final state is reached at point 5.

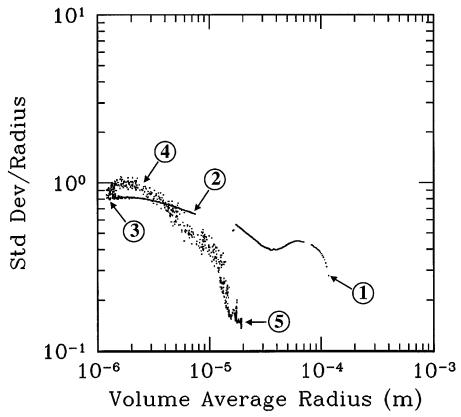

Fig. 6. Normalized standard deviation versus the volume average radius for the simulation shown of Fig. 2a. The numbers correspond to those in Fig. 2a.

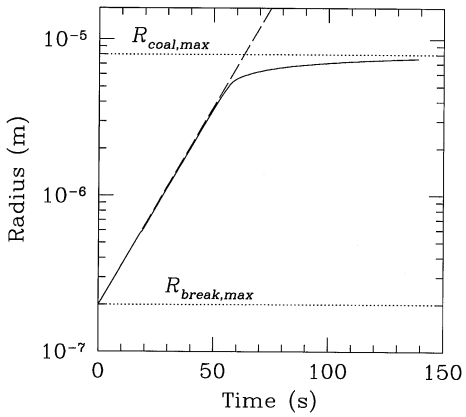

Fig. 7. Growth of the average size from $R_{\text{break,max}}$ to $R_{\text{coal,max}}$ for the case where all collisions result in coalescence events (----) and the case where a coalescence probability, (10), is used (—-) ($\mu_c = 1$ Pa s, $\mu_d = 1000$ Pa s, and $\sigma = 5 \times 10^{-3}$ N/m).

An estimate of the rate of decrease and increase in average size is given by the rates of stretching and coalescence. The time to reach $R_{\text{break,max}}$ can be estimated by using the average stretching rate.

$$t_{\min} \approx -\frac{2}{\dot{\lambda}_{\text{avg}}} \ln\left(\frac{R_{\text{break,max}}}{R_o}\right), \tag{11}$$

where $\dot{\lambda}_{\text{avg}}$ is the average stretching rate and R_o is the initial drop size.

The rate of increase in the average size can be estimated by the rate of coalescence, which is a function of the collision frequency and film drainage. Consider, as a first approximation, that all collisions result in a successful coalescence event. The rate of change in the number of drops is then given by the collision frequency which can be estimated using Smoluchowski's theory (see Levich, 1962)

$$\frac{\mathrm{d}n}{\mathrm{d}t} = -\frac{4\dot{\gamma}\phi n}{\pi}, \tag{12}$$

where n is the number of drops per unit volume. This approach is similar to that taken by Vinckier, Moldenaers, Terracciano, and Grizzuti (1998). Note that, among many assumptions, the above equation is for monodisperse drops, so as mixing proceeds the drop size changes and this equation is not completely accurate [The rate of collisions in a polydisperse system will be lower than that for a monodisperse system (Mishra, Kresta, & Masliyah, 1998).] As a first approximation, however, Eq. (12) is sufficient.

Substituting for n in terms of R_o and ϕ, gives an expression for the change in the average size, which can be solved for the time to go from $R_{\text{break,max}}$ to $R_{\text{coal,max}}$

$$t_{\max} = \frac{3\pi}{4\dot{\gamma}\phi} \ln\left(\frac{R_{\text{coal,max}}}{R_{\text{break,max}}}\right). \tag{13}$$

In reality, not all collisions result in a successful coalescence event. In order to account for this, the right side of (12) is multiplied by the coalescence probability (see (10)). Fig. 7 shows a comparison of growth in the average size for the cases assuming that all collisions result in coalescence and the case for including the coalescence probability. The initial size was taken to be $R_{\text{break,max}}$ and at long times the average size asymptotes to $R_{\text{coal,max}}$. At short times, there is essentially no difference between the two curves. Therefore, (13) can be used to obtain a reasonable estimate for the time to reach $R_{\text{coal,max}}$.

5. Conclusions

The following conditions serve to identify overemulsification:

$$\frac{R_{\text{def,min}}}{R_{\text{coal,max}}} > 1 \quad \text{and} \quad \frac{R_{\text{coal,max}}}{R_{\text{break,max}}} > 3. \tag{14}$$

Whether a steady state or oscillation occurs after the average size goes through a minimum is determined by the ratio of $R_{\text{def,min}}$ to $R_{\text{coal,max}}$.

$$\text{If } 1 < \frac{R_{\text{def,min}}}{R_{\text{coal,max}}} < 4 \;\Rightarrow\; \text{oscillation.} \tag{15a}$$

$$\text{If } 4 < \frac{R_{\text{def,min}}}{R_{\text{coal,max}}} \;\Rightarrow\; \text{steady state.} \tag{15b}$$

The values of $R_{\text{coal,max}}$, $R_{\text{def,min}}$, and $R_{\text{break,max}}$ are controlled by the material parameters (μ_c, μ_d, σ) and the process parameter ($\dot{\gamma}$). Thus, overemulsification can be induced by

- increasing p (decreasing μ_c and increasing μ_d),
- decreasing $\dot{\gamma}$,
- increasing σ.

More basic fluid mechanical work is needed to properly estimate the coefficients used in the inequalities 14 and 15.

Notation

A	Hamaker constant
Ca	$\mu_c \dot{\gamma} R/\sigma$, capillary number
$\mathrm{Ca}_{\mathrm{crit}}$	critical capillary number
F	force driving film drainage
h	film thickness during coalescence process
h_{crit}	critical film thickness at which rupture occurs
n	number of drops per unit volume
p	viscosity ratio
P	probability that a collision will result in a successful coalescence event
R_{avg}	volume average size of the drop distribution
$R_{\mathrm{break,max}}$	maximum size thread that can break in a given flow in a given time.
$R_{\mathrm{coal,max}}$	maximum size drop that can coalesce in a given flow.
$R_{\mathrm{def,min}}$	minimum size drop that can be deformed in a given flow.
R_o	original drop or thread size
s	standard deviation of the drop distribution
t_{break}	breakup time for a thread at rest
t_{max}	time needed to reach $R_{\mathrm{coal,max}}$ from $R_{\mathrm{def,min}}$
t_{min}	time needed to reach $R_{\mathrm{def,min}}$ from the initial drop size

Greek letters

α	collision angle
α_{crit}	critical collision angle
α_{init}	initial collision angle
α_0	initial amplitude of a disturbance during breakup at rest
ϕ	volume fraction of the dispersed phase
$\dot{\gamma}$	shear rate
$\dot{\lambda}$	average stretching rate
μ_c	viscosity of the continuous phase.
μ_d	viscosity of the dispersed phase.
σ	interfacial tension.
ω	collision frequency per unit volume per unit time
Ω_m	non-dimensional maximum growth rate of a disturbance during breakup at rest

Acknowledgements

This work was supported by the Department of Energy, Division of Basic Energy Sciences.

References

Adewole, A. A., Wolkowicz, M. D., Mascia, L., & Gogos, C. G. (1998). Morphology evolution and properties of physically and reactor compatibilized polypropylene–polystyrene blends. *SPE ANTEC Technical Papers*, *44*, 1489–1493.

Allan, R. S., & Mason, S. G. (1962). Particle motion in sheared suspensions—XIV. Coalescence of liquid drops in electric and shear fields. *Journal of Colloid Interface Science*, *17*, 383–408.

Becher, P. (1967). Effect of preparation parameters on the initial size distribution function in oil-in-water emulsions. *Journal of Colloid Interface Science*, *24*, 91–96.

Becher, P., & McCann, M. J. (1991). The process of emulsification: A computer model. *Langmuir*, *7*, 1325–1331.

Chesters, A. K. (1991). The modeling of coalescence processes in fluid–liquid dispersions: A review of current understanding. *Transactions of the Institute of Chemical Engineers*, *69*, 259–270.

DeRoussel, P., Khakhar, D. V., & Ottino, J. M. (2001). Mixing of viscous immiscible liquids. Part 1: Computational models for strong–weak and continuous flow systems. *Chemical Engineering Science*, *56*(19), 5511–5529.

Elemans, P. H. M., Bos, H. L., Janssen, J. M. H., & Meijer, H. E. H. (1993). Transient phenomena in dispersive mixing. *Chemical Engineering Science*, *48*, 267–276.

Grace, H. P. (1972). Dispersion phenomena in high viscosity immiscible fluid systems and application of static mixers as dispersion devices in such systems, *Third engineering foundation conference mixing*, *Andover*, *NH*, Republished 1982 in *Chemical Engineering Communicatons*, *14*, 225–227.

Grizzuti, N., & Bifulco, O. (1997). Effects of coalescence and breakup on the steady-state morphology of an immiscible polymer blend in shear flow. *Rheology Acta*, *36*, 406–415.

Janssen, J. M. H. (1993). *Dynamics of Liquid–Liquid Mixing*. Ph.D. Thesis, Eindhoven University of Technology.

Lachaise, J., Mendiboure, B., Dicharry, C., Marion, G., & Salager, J. L. (1996). Simulation of the overemulsification phenomenon in turbulent stirring. *Journal of Colloid Interface Science*, *110*, 1–10.

Levich, V. G. (1962). *Physicochemical hydrodynamics*. Englewood Cliffs, NJ, USA: Prentice-Hall.

Mishra, V., Kresta, S. M., & Masliyah, J. H. (1998). Self-preservation of the drop size distribution function and variation in the stability ratio for rapid coalescence of a polydisperse emulsion in a simple shear field. *Journal of Colloid Interface Science*, *197*, 57–67.

Taylor, G. I. (1934). The formation of emulsions in definable fields of flow. *Proceedings of the Royal Society of London*, *A143*, 501–532.

Tomotika, S. (1935). On the instability of a cylindrical thread of a viscous liquid surrounded by another viscous fluid. *Proceedings of the Royal Society*, *A150*, 322–337.

Tjahjadi, M., & Ottino, J. M. (1991). Stretching and breakup of droplets in chaotic flows. *Journal of Fluid Mechanics*, *232*, 191–219.

Vinckier, I., Moldenaers, P., Terracciano, A. M., & Grizzuti, N. (1998). Droplet size evolution during coalescence in semiconcentrated model blends. *A.I.Ch.E. Journal*, *44*, 951–958.